Qin *et al. Miner Miner Mater* 2023;2:9
DOI: 10.20517/mmm.2023.20

Minerals and Mineral Materials

Research Article

Open Access

3D montmorillonite aerogel/SA composite phase change materials with mechanically strong strength and superior thermal energy storage performances

Lei Qin[1], Cong Guo[1], Qijing Guo[1], Hao Yi[1,2], Feifei Jia[1,2]

[1]School of Resources and Environmental Engineering, Wuhan University of Technology, Wuhan 430070, Hubei, China.
[2]Hubei Key Laboratory of Mineral Resources Processing and Environment, Wuhan University of Technology, Wuhan 430070, Hubei, China.

Correspondence to: Dr. Hao Yi, School of Resources and Environmental Engineering, Wuhan University of Technology, 122 Luoshi Road, Wuhan 430070, Hubei, China. E-mail: yihao287@whut.edu.cn

How to cite this article: Qin L, Guo C, Guo Q, Yi H, Jia F. 3D montmorillonite aerogel/SA composite phase change materials with mechanically strong strength and superior thermal energy storage performances. *Miner Miner Mater* 2023;2:9. https://dx.doi.org/10.20517/mmm.2023.20

Received: 20 Jul 2023 **First Decision:** 21 Aug 2023 **Accepted:** 20 Sep 2023 **Published:** 28 Sep 2023

Academic Editors: Yaowen Xing, Lei Xie **Copy Editor:** Dong-Li Li **Production Editor:** Dong-Li Li

Abstract

Phase change materials (PCMs) often suffers leakage when used in thermal energy storage. In this work, for the sake of preventing leakage, three-dimensional interconnected montmorillonite aerogel (3D-Mt) has been designed through self-assembly method to encapsulate stearic acid (SA) as composite PCMs. The as prepared 3D-Mt with porous structure has encapsulated large amount of SA, which resulted in a high phase change enthalpy of 183 J/g. In addition, due to the surface tension and capillary forces of 3D-Mt aerogels, the SA were confined in the pore structure tightly, leading to excellent structural stability and good cycling performances during continuous solid-to-liquid phase change. In addition, due to the protection of 3D-Mt, the composite PCMs showed good shape stability and high mechanical strength. The prepared 3D-Mt/SA CPCMs can withstand a weight of 500 g without any deformation, and the loads are as high as 1.01 and 13.81 MPa under 55% and 80% deformation, respectively. With high heat storage capacity, good thermal stability, and excellent mechanical strength, the prepared 3D-Mt/SA CPCMs shows great application potential in the field of thermal energy storage.

Keywords: Montmorillonite, stearic acid, phase change materials, aerogel, mechanical strength

INTRODUCTION

With the growth of population, the process of urbanization, and the development of industrialization, the

consumption and demand for energy have surged dramatically[1-3]. Non-renewable energy sources, such as fossil fuels, have been overexploited, causing global warming and other serious environmental pollution[4,5]. In order to cope with the challenges from resource depletion and environmental contamination and solve the problem of mismatch between energy supply and demand, the utilization of sustainable energy is an important initiative[6-8]. Solar thermal energy has drawn considerable attention due to the characteristics of large reserves and no contamination, which can be used as an ideal alternative energy source[9,10]. The development and utilization of solar thermal energy is one of the most effective ways to deal with the shortage and depletion of traditional energy. Considering the intermittency, randomicity, and low energy density, which affect the utilization efficiency of solar thermal energy, it is of great significance to develop reliable, cost-effective solar energy collection and energy storage technologies[11,12]. Phase change materials (PCMs) can store/release heat by undergoing phase change in a small temperature range, which helps to improve energy utilization efficiency and is one of the ideal solutions to energy shortages and environmental problems[13,14]. Organic PCMs, such as stearic acid (SA), paraffin, polyethylene glycol (PEG), *etc*., with the advantages of high energy storage density, good chemical stability, and non-toxicity, have been widely studied and applied in thermal management fields such as building materials[15,16], solar energy storage[17-19], electronic equipment cooling[20,21], and industrial waste heat recovery[22,23] in recent years. SA is a kind of fatty acid widely existing in nature. It is widely used in PCMs[24,25], surfactants[26,27], pharmaceuticals[28,29], *etc*. It is considered to be a material with appropriate phase transition temperature and good latent heat capacity[30,31]. However, organic PCMs suffer from some challenges in the application, such as melting leakage, poor shape stability, and bad mechanical stability, which seriously limits the large-scale application of PCMs in the field of thermal management[32,33].

In order to solve the leakage problem of PCMs, some techniques have been developed, including microencapsulation[34,35] and shape stability technology. For example, Mohaddes *et al.* successfully used melamine-formaldehyde resin as the shell material to encapsulate n-eicosane, and the latent heat of melting of the microcapsules exceeded 162.4 J/g, which has good leakage resistance[36]. Li *et al.* encapsulated PEG in zirconium phosphate/polyvinyl alcohol composite aerogel by vacuum impregnation method, and the prepared composite PCMs (CPCMs) could maintain their shape stability during the PEG phase transition process[37]. Yang *et al.* combined self-assembly and chemical vapor deposition (CVD) technology to encapsulate hybrid graphene aerogel in graphene foam for encapsulation of paraffin[38], and the resulting CPCMs have good shape stability and high heat storage density[39]. Recently, it has been proved that CPCMs, supported by aerogels with high porosity, large specific surface area, and huge adsorption capacity, often show larger latent heat capacity while preventing leakage. However, most of the aerogel-based CPCMs have poor mechanical strength, which is liable to break under external force and lead to the risk of leakage. Therefore, exploring a simple and efficient method to prepare CPCMs with high heat storage performance and excellent mechanical properties is still a hot topic in the field of thermal management[40,41].

In this study, a mechanically strong aerogel has been designed to prepare CPCMs in order to improve shape stability. Montmorillonite (Mt) is a natural clay mineral with a layered structure that can be effortlessly exfoliated into 2D nanosheets. Besides, the Mt nanosheets can be easily assembled into aerogel under the action of a crosslinking agent. In previous literature, it turned out that the addition of Mt in the organic aerogel can greatly promote the mechanical strength (Biswas *et al*., 2019)[42]. At the same time, sodium alginate is a general crosslinking agent that can be used to synthesize organic aerogel. As a consequence, the mechanically strong aerogel is designed through a self-assembled method by using Mt integrated with sodium alginate; the obtained aerogel with abundant pores can encapsulate a large amount of PCMs and lead to large latent heat capacity. Besides, the addition of Mt can reinforce the mechanical strength of the Mt aerogel and the CPCMs, which will benefit the shape stability and cycling performances of the CPCMs[24]. In

addition, the obtained CPCMs can effectively prevent leakages during solid-to-liquid phase change owing to surface tension and capillary forces of the 3D-Mt aerogel. The innovation of this study is to prepare a Mt-based CPCM with excellent mechanical properties, which solves the problem of poor mechanical strength and takes into account the high heat storage performance. The strong mechanical strength, excellent thermal storage behavior, and good structure stability of the CPCMs are highlighted in this study. Having solved the mechanical strength of the aerogel-based CPCMs and improved thermal energy storage performances, the designed CPCMs show great potential in renewable energy and sustainable development fields.

METHODS

Materials

SA, sodium alginate, calcium chloride ($CaCl_2$), and absolute ethanol (C_2H_6O, 99.7%) were purchased from Shanghai Sinopharm Chemical Reagent Co., Ltd. All chemicals were used without further purification. Mt was acquired from Chifeng Ningcheng Montmorillonite Company Limited (Inner Mongolia, China). Deionized water, produced by a Milli-Q ultra-pure water meter (Milli-Q, US) with a resistivity of 18.2 MΩ·cm, was used in all experiments.

Preparation of 3D-Mt/SA CPCMs

3D-Mt/SA CPCMs are prepared by vacuum impregnation, and the specific preparation steps are as follows: First, 5 g of Mt was added to 100 mL of deionized water and was stirred for 10 min at 25 °C. Subsequently, 5 g of SA was uniformly dispersed in the suspension while continuing the stirring for 10 min. The mixtures were freeze-dried for 12 h, and then the freeze-dried sample was soaked in 49 g of ethanol solution containing 1 g of $CaCl_2$ for 6 h and subjected to Ca^{2+} crosslinking to enhance the mechanical strength. 3D-Mt aerogels were obtained after evaporating the alcohol in an oven at 60 °C. Subsequently, a sufficient amount of SA and 3D-Mt aerogels were placed in a vacuum drying oven at 80 °C for 3 h to make the molten SA reach adsorption saturation in 3D-Mt aerogels. After vacuum impregnation, the 3D-Mt/SA CPCMs were placed on filter paper in an atmosphere of 80 °C to remove excess SA.

Characterization

Fourier transform infrared spectroscopy (FTIR, Nicolet 6700) was used to analyze the chemical structure of samples and the compatibility between components in the wavelength range of 400-4,000 cm^{-1}. The X-ray diffraction patterns of the samples were obtained by X-ray diffractometer (XRD, Bruker, Germany). The morphology and structure of the samples before and after vacuum impregnation were characterized by scanning electron microscopy (SEM, Phenom ProX) at an accelerating voltage of 15 kV. A differential scanning calorimeter (DSC, Discovery DSC25 - TA Instruments) was used to investigate the thermal properties of the samples at a heating/cooling rate of 2 °C/min under a nitrogen atmosphere. Thermogravimetric (TG) analysis of samples is performed via a thermal analyzer (NETZSCH STA 449 F5) from room temperature to 600 °C to investigate the thermal stability of the sample. An infrared camera (FOTRIC 224s) was used to record the temperature change of the sample during the heat storage process, and in this test, a xenon lamp was used to simulate sunlight to provide a heat source. Microcomputer-controlled electro-hydraulic servo universal testing machine (SHT4106) is used to study the mechanical strength of samples.

RESULTS AND DISCUSSION

Structural morphology of 3D-Mt/SA CPCMs

The morphology of 3D-Mt/SA CPCMs was studied by SEM. As shown in Figure 1A, it can be observed that the 3D-Mt aerogels have interconnected sheet-like porous structures, providing a large amount of adsorption space for the molten PCMs, which is responsible for better thermal storage properties per unit

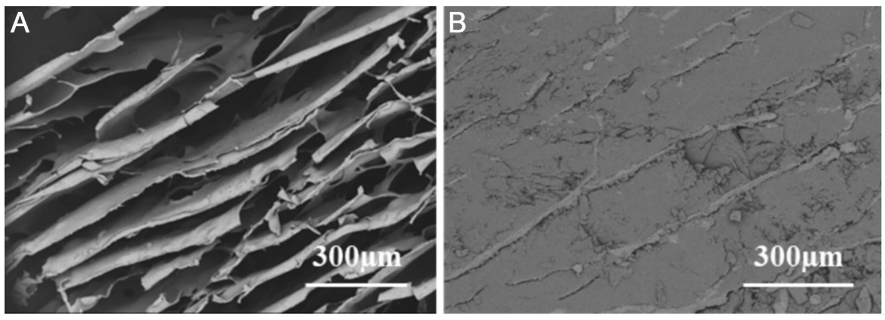

Figure 1. SEM images of (A) 3D-Mt aerogels and (B) 3D-Mt/SA CPCMs. CPCMs: Composite phase change materials; Mt: montmorillonite; SA: stearic acid; SEM: scanning electron microscopy.

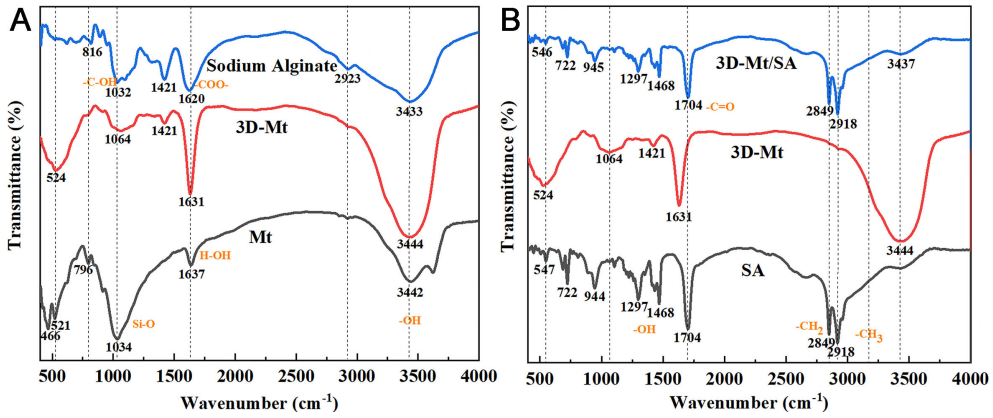

Figure 2. (A) FTIR spectra of Mt, sodium alginate, and 3D-Mt aerogels; (B) FTIR spectra of SA, 3D-Mt, and 3D-Mt/SA CPCMs. CPCMs: Composite phase change materials; FTIR: fourier transform infrared spectroscopy; Mt: montmorillonite; SA: stearic acid.

volume. As shown in Figure 1B, in the structure of 3D-Mt/SA CPCMs, SA is embedded and uniformly dispersed in the porous network structure of 3D-Mt aerogels. The porous structure of 3D-Mt aerogels provides surface tension and capillary forces to confine molten SA in the pore structure with the purpose of preventing leakage.

Synthesis mechanism of 3D-Mt/SA PCMs

The interaction of each component affects the latent heat storage performance of 3D-Mt/SA CPCMs, so the synthesis mechanism of 3D-Mt/SA CPCMs has been studied by FTIR. Figure 2A shows the FTIR spectra of Mt, sodium alginate, and 3D-Mt aerogels. In the spectrum of Mt, the broad absorption band at 3,442 cm^{-1} corresponds to the O-H stretching vibration[43]; the recorded peak at 1,637 cm^{-1} is attributed to the bending vibration of the H-OH bond[44] (Brahmi *et al.*, 2021). The peak at 1,034 cm^{-1} is caused by the stretching vibration of Si-O; the absorption peaks at 521 and 466 cm^{-1} are usually related to the bending vibration of Si-O-Al and Si-O-Si[45]. As for sodium alginate, the peak at 3,433 cm^{-1} is related to the stretching vibration of the hydroxyl group (-OH). The peaks at 1,620 and 1,421 cm^{-1} represent the stretching vibration of the carboxyl group (-COO-); the absorption peak at 1,032 cm^{-1} corresponds to the stretching vibration of the alcohol group (-C-OH) (Peng *et al.*, 2017)[45]. In the spectrum of 3D-Mt aerogels, the stretching vibration of the -COO- group (1,620 cm^{-1}) in sodium alginate and the bending vibration of the H-OH bond (1,637 cm^{-1}) in Mt overlap at 1,631 cm^{-1}, which suggests that the hydrogen bond has been formed between Mt and sodium alginate[46,47].

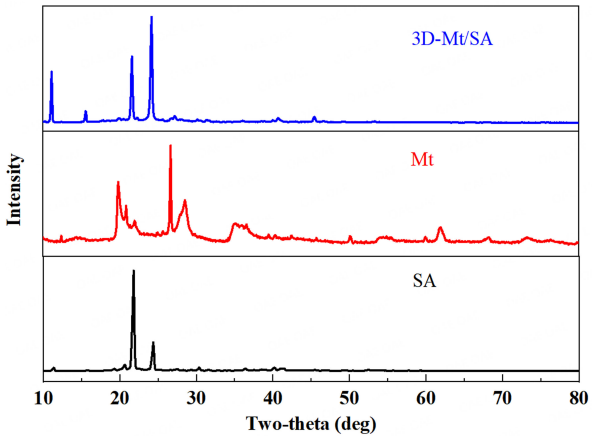

Figure 3. XRD spectra of SA, Mt, and 3D-Mt/SA CPCMs. CPCMs: Composite phase change materials; Mt: montmorillonite; SA: stearic acid; XRD: X-ray diffractometer.

The chemical compatibility of SA and 3D-Mt aerogels was further studied. Figure 2B shows the FTIR spectra of 3D-Mt/SA CPCMs, SA, and 3D-Mt aerogels. In the pure SA spectrum, the absorption peaks at wavenumbers 2,918 and 2,849 cm^{-1} correspond to the symmetric stretching vibrations of $-CH_3$ and $-CH_2$, respectively. The strong absorption peak at 1,704 cm^{-1} represents the stretching vibration of C=O[45,48,49]. The peaks at 1,468 and 1,297 cm^{-1} are the absorption peaks of the in-plane bending vibration of -OH functional group; the peaks at 944 and 722 cm^{-1} are attributed to the out-of-plane bending vibration and in-plane rocking vibration of -OH functional group, respectively[50-53]. In the spectra of 3D-Mt/SA CPCMs, all absorption peaks correspond to SA and 3D-Mt aerogels, and no new peaks are generated. This result indicated that no chemical reaction occurred between SA and 3D-Mt aerogels. The molten SA is adsorbed in the pores of the 3D-Mt aerogels through capillary and surface tension.

Chemical compatibility of 3D-Mt/SA CPCMs

By comparing the XRD patterns of 3D-Mt/SA CPCMs with Mt and SA, it is further judged and analyzed whether the components in CPCMs undergo chemical reactions to produce new substances. Figure 3 shows the XRD spectra of SA, Mt, and 3D-Mt/SA CPCMs. It can be seen from the figure that pure SA has two strong diffraction peaks at $2\theta = 21.8°$ and $2\theta = 24.3°$ and a weak diffraction peak at $2\theta = 11.4°$. In the XRD spectra of 3D-Mt/SA CPCMs, the diffraction peaks are mainly caused by the crystallization of SA components, and the peaks observed at $2\theta = 21.8°$ and $2\theta = 24.3°$ overlap with the characteristic peaks of SA. However, the peak intensity at $2\theta = 21.8°$ decreased, which was mainly attributed to the smaller crystallite size of SA in CPCMs due to the confinement of aerogel pore structure[54,55]. XRD results showed that the 3D-Mt/SA CPCMs had a high degree of crystallinity, the SA was in a crystalline state even after combination, suggesting good chemical compatibility between the SA and 3D-Mt, and the components were only combined in a physical form.

Mechanical strength of 3D-Mt/SA CPCMs

High mechanical strength is one of the necessary conditions for 3D-Mt/SA CPCMs to maintain structural stability in practical applications, so this experiment explored the mechanical stability of the material. Mt, as a supporting frame, can enhance the stability of the structure[56]. As shown in Figure 4A, the 3D-Mt/SA CPCMs did not undergo obvious deformation after placing the weights of 100 and 500 g on the upper surface of 3D-Mt/SA CPCMs, and no cracks were observed. Stress-strain tests were further carried out, and the results are shown in Figure 4B. The stress-strain curves of 3D-Mt/SA CPCMs can be divided into three parts: at low strains of < 5% corresponding to rigid elastic deformation; the strain between 5% and 55% is the

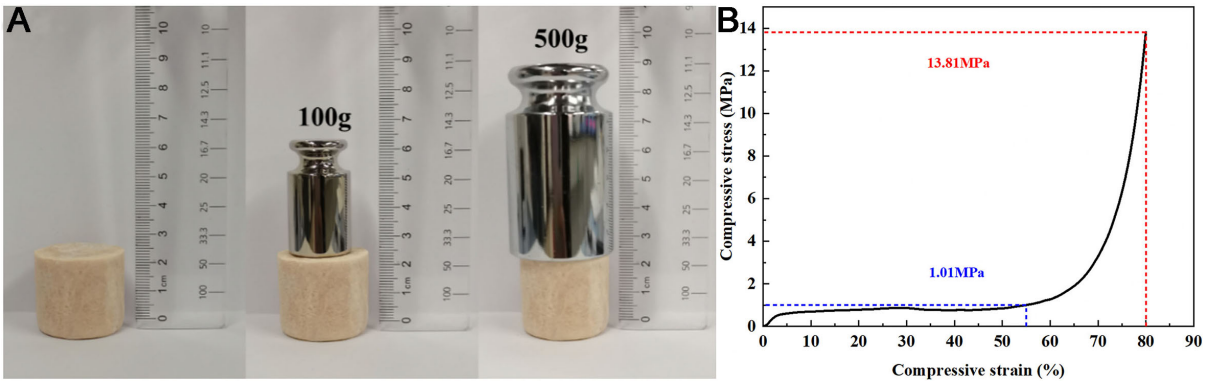

Figure 4. (A) 3D-Mt/SA CPCMs under different weight loads; (B) Compressive stress-strain curve of 3D-Mt/SA CPCMs. CPCMs: Composite phase change materials; Mt: montmorillonite; SA: stearic acid.

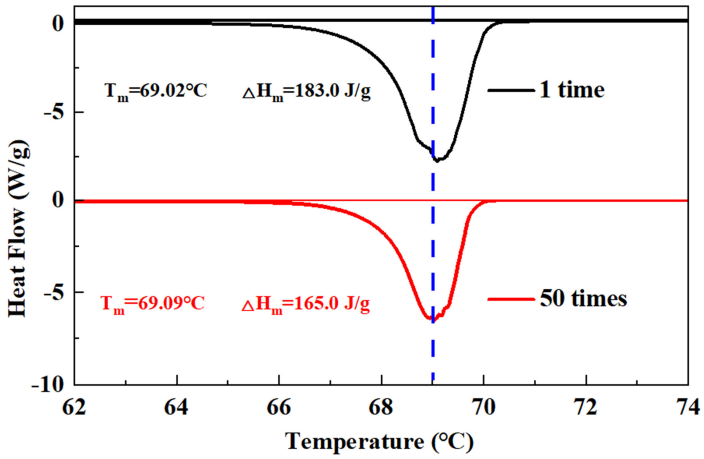

Figure 5. TG curves of pure SA, 3D-Mt, and 3D-Mt/SA CPCMs. CPCMs: Composite phase change materials; Mt: montmorillonite; SA: stearic acid; TG: thermogravimetric.

plastic deformation platform; high strains of > 55% lead to an exponential increase in stress per strain due to plastic deformation and densification, implying the loss of the characteristic 3D interconnected network structure of 3D-Mt/SA CPCMs. The results showed that the 3D-Mt/SA CPCMs exhibited excellent mechanical strength with loads of 1.01 MPa at 55% strain and 13.81 MPa at 80% strain.

Thermal stability and shape stability of 3D-Mt/SA CPCMs

Thermal stability is an important factor for the practical application of 3D-Mt/SA CPCMs, and the thermal degradation temperature of 3D-Mt/SA CPCMs and their components were determined by TG analysis. Figure 5 shows the TG curves of pure SA, Mt, and 3D-Mt/SA CPCMs. The results showed that there was a one-step thermal decomposition process of SA in the range of 200-320 °C, and the slight weight loss of Mt below 100 °C was attributed to the evaporation of adsorbed water. In the TG curves of 3D-Mt/SA CPCMs, a decomposition trend was shown to be similar to that of pure SA. At temperatures below 320 °C, most of the weight loss was attributed to the removal of SA in the composites, and the weight loss at temperatures above 320 °C was mainly due to the degradation of the main chain of SA in aerogels. In addition, the onset temperature of weight loss of 3D-Mt/SA CPCMs is lower than that of pure SA, which is mainly attributed to the thermal conduction path provided by the aerogel framework, which accelerates the decomposition of

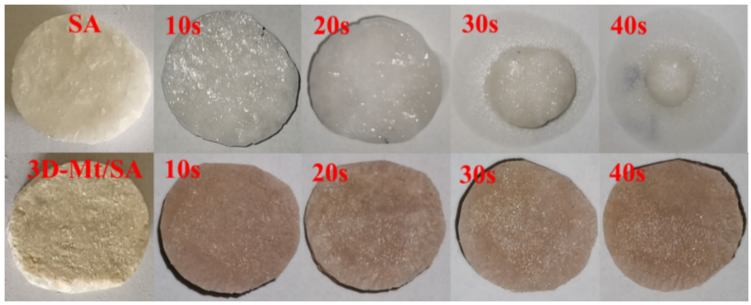

Figure 6. Shape pictures of pure SA and 3D-Mt/SA CPCMs heated for varying durations. CPCMs: Composite phase change materials; Mt: montmorillonite; SA: stearic acid.

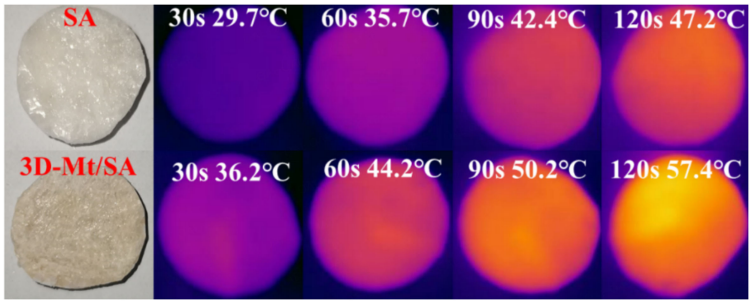

Figure 7. Infrared thermography images of pure SA and 3D-Mt/SA CPCMs. CPCMs: Composite phase change materials; Mt: montmorillonite; SA: stearic acid.

SA. The comparison of the threshold temperature of stability in our work and other composites is listed in Table 1. It can be observed that the 3D-Mt/SA CPCMs have good thermal stability.

In order to explore the shape stability of 3D-Mt/SA CPCMs, the anti-leakage test was carried out. Figure 6 shows the shape pictures of pure SA and 3D-Mt/SA CPCMs heated on a 90 °C heating plate for various durations. It can be seen from the photo that pure SA melts quickly during the heating process and basically melts into a liquid after heating for 40 s. After heating, the surface of 3D-Mt/SA CPCMs was wetted, but almost no liquid leaked out on the filter paper. 3D-Mt aerogels provide a strong 3D framework structure for SA, which can confine the molten SA in the pore structure, which is beneficial to preventing leakage. The results show that the 3D-Mt/SA CPCMs have excellent shape stability and can maintain their shape even at high temperatures.

Thermal energy storage properties of 3D-Mt/SA CPCMs

The temperature response speed determines the heat storage/release efficiency of PCMs. In this experiment, a heat source is provided above the sample by xenon lamp light, and the thermal response of the sample is evaluated by monitoring the temperature change of the sample by an infrared camera. The results are shown in Figure 7; the temperature of pure SA increased from room temperature to 29.7 °C after 30 s of light irradiation, while that of 3D-Mt/SA CPCMs increased to 36.2 °C. After 120 s of light irradiation, 3D-Mt/SA CPCMs increased to 57.4 °C, which was 10.2 °C higher than that of pure SA. This phenomenon is attributed to the fact that the 3D structure of 3D-Mt aerogels provides a heat transfer path, which enhances the heat transfer performance and ensures the rapid heat storage of 3D-Mt/SA CPCMs, making it an ideal choice for efficient thermal energy storage.

Table 1. Comparison of the threshold temperature of stability of 3D-Mt/SA CPCMs with other composites

CPCMs	Threshold temperature of stability (°C)	Ref.
Atapulgite/Capric-Myristic acid eutectic mix composite	156	[57]
Eutectic mixture/Expanded graphite	160	[58]
Ddecylamine/Crbonized clay/pectin aerogels	150	[59]
3D-Mt/SA CPCMs	200	This work

CPCMs: Composite phase change materials; Mt: montmorillonite; SA: stearic acid.

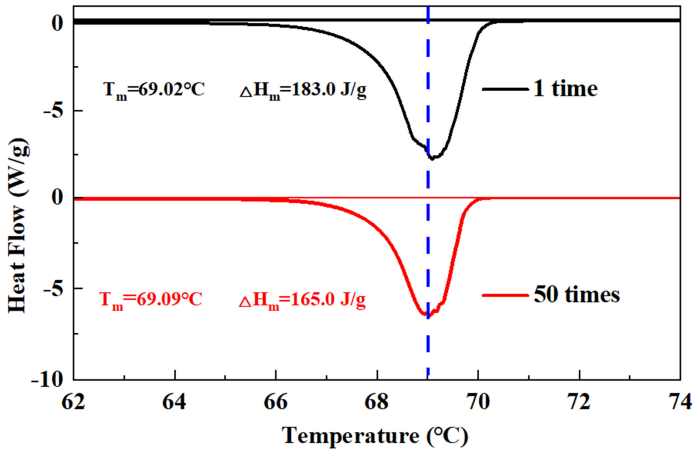

Figure 8. Cycle stability of 3D-Mt/SA CPCMs. CPCMs: Composite phase change materials; Mt: montmorillonite; SA: stearic acid.

Phase change performance and cycle stability are the key parameters affecting the practical application of 3D-Mt/SA CPCMs. CPCMs continuously undergo phase transitions under heat storage and release conditions, and the storage state of SA in 3D-Mt aerogels is also changing, which will have a certain impact on the heat storage and heat release properties of the materials. The 3D-Mt/SA CPCMs were heated on a 90 °C heating plate for 40 s and 50 cycles of heating/cooling experiments were performed. Figure 8 shows the DSC curves of 3D-Mt/SA CPCMs before and after 50 cycles, comparing the data after 50 cycles with the data before the cycle. The results showed that the melting latent heat of 3D-Mt/SA CPCMs decreased from 183.0 to 165.0 J/g. The slight decrease in latent heat is attributed to the loss of a small amount of molten SA in the outer layer of 3D-Mt/SA CPCMs, and the decrease in latent heat value is within the appropriate range of the application. After continuous melting and freezing cycles, 3D-Mt/SA CPCMs can maintain reversible phase transition without deterioration of phase change performance, so 3D-Mt/SA CPCMs have good cycle stability and can be reused for heat storage. The relevant results of some clay-based CPCMs are compared. It can be observed from Table 2 that the loading ratio and latent heat capacity of the 3D-Mt / SA CPCMs in this study have certain advantages. The Mass ratio and heat storage capacity of the CPCMs have been improved. In addition, the 3D-Mt/SA CPCMs have good mechanical strength and good application potential.

In conclusion, a method for preparing 3D-Mt/SA CPCMs with excellent mechanical strength and heat storage is provided. In these CPCMs, 3D-Mt aerogels were used as a support material to encapsulate SA, which effectively solved the main problem of easy leakage of PCMs. The melting enthalpy of 3D-Mt/SA CPCMs is as high as 183 J/g, and it can be kept stable for 50 melting/freezing cycles, showing an excellent

Table 2. Comparison of latent heat of 3D-Mt/SA CPCMs with previous clay-based CPCMs

CPCMs	PCMs mass rate (%)	Latent heat (J/g)	Ref.
Kaolinite/paraffin	50.9	107.2	[60]
Diatomite/$CH_3COONa\ 3H_2O$	63	168.3	[61]
Na-Mt/Paraffinic	31.82	78.78	[62]
OMt/Paraffin	37.1	51.8	[63]
Sepiolite/$CaCl_2{\cdot}6H_2O$	70	87.9	[64]
3D-Mt/SA CPCMs	85.09	183.0	This work

CPCMs: Composite phase change materials; Mt: montmorillonite; PCMs: phase change materials; SA: stearic acid.

heat storage effect. In addition, the prepared 3D-Mt/SA CPCMs can withstand a weight of 500 g without any deformation, and the loads are as high as 1.01 and 13.81 MPa under 55% and 80% deformation, respectively, showing excellent mechanical properties. Based on the high heat storage capacity, excellent mechanical strength, and thermal stability of 3D-Mt/SA CPCMs, these CPCMs possess great potential for applications in thermal energy management and conversion systems in complex environments.

DECLARATIONS

Authors' contributions

Conceptualization, methodology, investigation, writing, review and editing: Qin L, Guo C
Methodology, investigation: Guo Q
Conceptualization, review and editing, technical, and material support: Yi H, Jia F

Availability of data and materials

Not applicable.

Financial support and sponsorship

This work was supported by the National Natural Science Foundation of China (52104265).

Conflicts of interest

All authors declared that there are no conflicts of interest.

Ethical approval and consent to participate

Not applicable.

Consent for publication

Not applicable.

REFERENCES

1. Dubey AK, Sun J, Choudhary T, et al. Emerging phase change materials with improved thermal efficiency for a clean and sustainable environment: an approach towards net zero. *Renew Sust Energy Rev* 2023;182:113421. DOI
2. Nematchoua MK, Noelson JCV, Saadi I, et al. Application of phase change materials, thermal insulation, and external shading for thermal comfort improvement and cooling energy demand reduction in an office building under different coastal tropical climates. *Solar Energy* 2020;207:458-70. DOI
3. Zhang J, Sajadi SM, Chen Y, Tlili I, Fagiry MA. Effects of Al_2O_3 and TiO_2 nanoparticles in order to reduce the energy demand in the conventional buildings by integrating the solar collectors and phase change materials. *Sustain Energy Technol Assess* 2022;52:102114.

DOI
4. Suraparaju SK, Natarajan SK, Mamilla VR, Pappala SMT, Kurada A, Lakamsani MSVP. Energy, exergy, economic and environmental (4E) analyses of solar still with paraffin wax as phase change energy storage material. *Mater Today Proc* 2023;90:1-5. DOI
5. Zhao S, Yuan A, Xu H, et al. Elevating the photothermal conversion efficiency of phase-change materials simultaneously toward solar energy storage, self-healing, and recyclability. *ACS Appl Mater Interfaces* 2022;14:29213-22. DOI
6. Aftab W, Usman A, Shi J, Yuan K, Qin M, Zou R. Phase change material-integrated latent heat storage systems for sustainable energy solutions. *Energy Environ Sci* 2021;14:4268-91. DOI
7. Gong B, Yang H, Wu S, et al. Phase change material enhanced sustained and energy-efficient solar-thermal water desalination. *Appl Energy* 2021;301:117463. DOI
8. Tuly SS, Islam MS, Hassan R, Das BK, Sarker MRI. Investigation of a modified double slope solar still integrated with nanoparticle-mixed phase change materials: energy, exergy, exergo-economic, environmental, and sustainability analyses. *Case Stud Therm Eng* 2022;37:102256. DOI
9. Chen Y, He H, Li J, He H, Chen S, Deng C. Waste sugarcane skin-based composite phase change material for thermal energy storage and solar energy utilization. *Mater Lett* 2023;342:134320. DOI
10. Li X, Liu Y, Xu Y, Tao P, Deng T. Solid-liquid phase change composite materials for direct solar-thermal energy harvesting and storage. *Acc Mater Res* 2023;4:484-95. DOI
11. da Cunha SRL, de Aguiar JLB. Phase change materials and energy efficiency of buildings: a review of knowledge. *J Energy Storage* 2020;27:101083. DOI
12. Singh P, Sharma RK, Ansu AK, Goyal R, Sarı A, Tyagi VV. A comprehensive review on development of eutectic organic phase change materials and their composites for low and medium range thermal energy storage applications. *Sol Energy Mater Sol Cells* 2021;223:110955. DOI
13. Arıcı M, Bilgin F, Nižetić S, Karabay H. PCM integrated to external building walls: an optimization study on maximum activation of latent heat. *Appl Therm Eng* 2020;165:114560. DOI
14. Hossain MS, Pandey AK, Selvaraj J, Rahim NA, Islam MM, Tyagi VV. Two side serpentine flow based photovoltaic-thermal-phase change materials (PVT-PCM) system: energy, exergy and economic analysis. *Renew Energy* 2019;136:1320-36. DOI
15. Liu Z, Yu Z(J), Yang T, et al. A review on macro-encapsulated phase change material for building envelope applications. *Build Environ* 2018;144:281-94. DOI
16. Ma Y, Li D, Yang R, et al. Energy and daylighting performance of a building containing an innovative glazing window with solid-solid phase change material and silica aerogel integration. *Energy Convers Manag* 2022;271:116341. DOI
17. Liu H, Wang X, Wu D, Ji S. Fabrication and applications of dual-responsive microencapsulated phase change material with enhanced solar energy-storage and solar photocatalytic effectiveness. *Sol Energy Mater Sol Cells* 2019;193:184-97. DOI
18. Liu J, Zou X, Cai Z, Peng Z, Xu Y. Polymer based phase change material for photo-thermal utilization. *Sol Energy Mater Solar Cells* 2021;220:110852. DOI
19. Sun K, Dong H, Kou Y, et al. Flexible graphene aerogel-based phase change film for solar-thermal energy conversion and storage in personal thermal management applications. *Chem Eng J* 2021;419:129637. DOI
20. Wang M, Zhang C, Wang J, Wang Y, Yu F. Carbon hybrid aerogel-based phase change material with reinforced energy storage and electro-thermal conversion performance for battery thermal management. *J Energy Storage* 2022;52:104905. DOI
21. Wang X, Li G, Hong G, Guo Q, Zhang X. Graphene aerogel templated fabrication of phase change microspheres as thermal buffers in microelectronic devices. *ACS Appl Mater Interfaces* 2017;9:41323-31. DOI PubMed
22. Gong S, Li X, Sheng M, et al. High thermal conductivity and mechanical strength phase change composite with double supporting skeletons for industrial waste heat recovery. *ACS Appl Mater Interfaces* 2021;13:47174-84. DOI PubMed
23. Shon J, Kim H, Lee K. Improved heat storage rate for an automobile coolant waste heat recovery system using phase-change material in a fin-tube heat exchanger. *Appl Energy* 2014;113:680-9. DOI
24. Li D, Cheng X, Li Y, et al. Effect of MOF derived hierarchical Co_3O_4/expanded graphite on thermal performance of stearic acid phase change material. *Sol Energy* 2018;171:142-9. DOI
25. Yi H, Ai Z, Zhao Y, Zhang X, Song S. Design of 3D-network montmorillonite nanosheet/stearic acid shape-stabilized phase change materials for solar energy storage. *Sol Energy Mater Sol Cells* 2020;204:110233. DOI
26. Bhadani A, Iwabata K, Sakai K, Koura S, Sakai H, Abe M. Sustainable oleic and stearic acid based biodegradable surfactants†. *RSC Adv* 2017;7:10433-42. DOI
27. Dong Q, Li X, Dong J. Synthesis of branched surfactant via ethoxylation of oleic acid derivative and its surface properties. *Chem Eng Sci* 2022;258:117747. DOI
28. Massias T, de Paiva Lacerda S, de Azevedo JR, et al. A proof-of-concept study of coupled supercritical CO2-assisted processes to produce solid self-assembled drug delivery systems (S-SADDS). *J Cryst Growth* 2023;616:127245. DOI
29. Yaglioglu A, Yaglioglu MS, Tosyalıoglu N, Adem S, Demirtas I. Chemical profiling, *in vitro* biological activities and Pearson correlation between chemical profiling and anticancer activities of four Abies species from Turkey. *S Afr J Bot* 2022;151:600-13. DOI
30. Wang B, Shi M, Yao H, et al. Preparation and application of low-temperature binary eutectic lauric acid-stearic acidSiO_2 phase change microcapsules. *Energy Build* 2023;279:112706. DOI
31. Zhou Y, Cao Y, Chen H, et al. Three-dimensional continuous network graphite nanosheets-based carbon foam supported stearic acid

as effective shape-stabilized phase change material. *J Energy Storage* 2023;59:106575. DOI
32. Mohamed SA, Al-sulaiman FA, Ibrahim NI, et al. A review on current status and challenges of inorganic phase change materials for thermal energy storage systems. *Renew Sust Energy Rev* 2017;70:1072-89. DOI
33. Su W, Darkwa J, Kokogiannakis G. Review of solid-liquid phase change materials and their encapsulation technologies. *Renew Sust Energy Rev* 2015;48:373-91. DOI
34. Cao L, Tang F, Fang G. Preparation and characteristics of microencapsulated palmitic acid with TiO_2 shell as shape-stabilized thermal energy storage materials. *Sol Energy Mater Sol Cells* 2014;123:183-8. DOI
35. Chang Z, Wang K, Wu X, et al. Review on the preparation and performance of paraffin-based phase change microcapsules for heat storage. *J Energy Storage* 2022;46:103840. DOI
36. Mohaddes F, Islam S, Shanks R, Fergusson M, Wang L, Padhye R. Modification and evaluation of thermal properties of melamine-formaldehyde/n-eicosane microcapsules for thermo-regulation applications. *Appl Therm Eng* 2014;71:11-5. DOI
37. Li W, Zhai D, Gu Y, et al. 3D zirconium phosphate/polyvinyl alcohol composite aerogels for form-stable phase change materials with brilliant thermal energy storage capability. *Sol Energy Mater Sol Cells* 2022;239:111681. DOI
38. Yang J, Qi GQ, Bao RY, et al. Hybridizing graphene aerogel into three-dimensional graphene foam for high-performance composite phase change materials. *Energy Storage Mater* 2018;13:88-95. DOI
39. Luo Y, Xie Y, Jiang H, et al. Flame-retardant and form-stable phase change composites based on MXene with high thermostability and thermal conductivity for thermal energy storage. *Chem Eng J* 2021;420:130466. DOI
40. Wu H, Li S, Shao Y, et al. Melamine foam/reduced graphene oxide supported form-stable phase change materials with simultaneous shape memory property and light-to-thermal energy storage capability. *Chem Eng J* 2020;379:122373. DOI
41. Xue F, Lu Y, Qi X, Yang J, Wang Y. Melamine foam-templated graphene nanoplatelet framework toward phase change materials with multiple energy conversion abilities. *Chem Eng J* 2019;365:20-9. DOI
42. Biswas B, Warr LN, Hilder EF, et al. Biocompatible functionalisation of nanoclays for improved environmental remediation. *Chem Soc Rev* 2019;48:3740-70. DOI
43. Shabanpour S, Shariati FP, Khatibani AB. Potential Alendronate Sodium drug carrier by preparation and characterization of sodium alginate cross-linked Montmorillonite. *Braz J Pharm Sci* 2022;58:e20243. DOI
44. Brahmi M, Essifi K, Elbachiri A, Tahani A. Adsorption of sodium alginate onto sodium montmorillonite. *Mater Today Proc* 2021;45:7789-93. DOI
45. Peng K, Fu L, Li X, Ouyang J, Yang H. Stearic acid modified montmorillonite as emerging microcapsules for thermal energy storage. *Appl Clay Sci* 2017;138:100-6. DOI
46. Daemi H, Barikani M. Synthesis and characterization of calcium alginate nanoparticles, sodium homopolymannuronate salt and its calcium nanoparticles. *Sci Iran* 2012;19:2023-8. DOI
47. Wang W, Zhao Y, Bai H, Zhang T, Ibarra-Galvan V, Song S. Methylene blue removal from water using the hydrogel beads of poly(vinyl alcohol)-sodium alginate-chitosan-montmorillonite. *Carbohydr Polym* 2018;198:518-28. DOI PubMed
48. Wang L, Yu G, Li J, et al. Stretchable hydrophobic modified alginate double-network nanocomposite hydrogels for sustained release of water-insoluble pesticides. *J Clean Prod* 2019;226:122-32. DOI
49. Zhang M, Chen H. Development and characterization of starch-sodium alginate-montmorillonite biodegradable antibacterial films. *Int J Biol Macromol* 2023;233:123462. DOI
50. Chen Z, Cao L, Shan F, Fang G. Preparation and characteristics of microencapsulated stearic acid as composite thermal energy storage material in buildings. *Energy Build* 2013;62:469-74. DOI
51. Fang G, Li H, Chen Z, Liu X. Preparation and characterization of stearic acid/expanded graphite composites as thermal energy storage materials. *Energy* 2010;35:4622-6. DOI
52. Tahan Latibari S, Mehrali M, Mehrali M, et al. Facile synthesis and thermal performances of stearic acid/titania core/shell nanocapsules by sol-gel method. *Energy* 2015;85:635-44. DOI
53. Tang F, Cao L, Fang G. Preparation and thermal properties of stearic acid/titanium dioxide composites as shape-stabilized phase change materials for building thermal energy storage. *Energy Build* 2014;80:352-7. DOI
54. Ionita M, Pandele MA, Iovu H. Sodium alginate/graphene oxide composite films with enhanced thermal and mechanical properties. *Carbohydr Polym* 2013;94:339-44. DOI PubMed
55. Verma A, Thakur S, Mamba G, et al. Graphite modified sodium alginate hydrogel composite for efficient removal of malachite green dye. *Int J Biol Macromol* 2020;148:1130-9. DOI
56. Yi H, Xia L, Song S. Three-dimensional montmorillonite/Ag nanowire aerogel supported stearic acid as composite phase change materials for superior solar-thermal energy harvesting and storage. *Compos Sci Technol* 2022;217:109121. DOI
57. Gencel O, Ustaoglu A, Benli A, et al. Investigation of physico-mechanical, thermal properties and solar thermoregulation performance of shape-stable attapulgite based composite phase change material in foam concrete. *Sol Energy* 2022;236:51-62. DOI
58. Alkhazaleh AH, Almanaseer W, Ismail M, Almashaqbeh S, Farid MM. Thermal and mechanical properties of cement based-composite phase change material of butyl stearate/isopropyl palmitate/expanded graphite for low temperature solar thermal applications. *J Energy Storage* 2022;50:104547. DOI
59. Wang L, Liang W, Liu Y, et al. Carbonized clay pectin-based aerogel for light-to-heat conversion and energy storage. *Appl Clay Sci* 2022;224:106524. DOI
60. Li C, Fu L, Ouyang J, Tang A, Yang H. Kaolinite stabilized paraffin composite phase change materials for thermal energy storage.

Appl Clay Sci 2015;115:212-20. DOI

61. Yang Z, Yang Z, Li J, et al. Design of diatomite-based hydrated salt composites with low supercooling degree and enhanced heat transfer for thermal energy storage. *Int J Energy Res* 2019;43:7058-74. DOI
62. Jeong SG, Jin Chang S, We S, Kim S. Energy efficient thermal storage montmorillonite with phase change material containing exfoliated graphite nanoplatelets. *Sol Energy Mater Sol Cells* 2015;139:65-70. DOI
63. Li M, Guo Q, Nutt S. Carbon nanotube/paraffin/montmorillonite composite phase change material for thermal energy storage. *Sol Energy* 2017;146:1-7. DOI PubMed PMC
64. Cui W, Zhang H, Xia Y, et al. Preparation and thermophysical properties of a novel form-stable $CaCl_2 \cdot 6H_2O$/sepiolite composite phase change material for latent heat storage. *J Therm Anal Calorim* 2018;131:57-63. DOI